Mikailalsys Journal of Advanced Engineering International

e-ISSN : 3046-9694
p-ISSN : 3046-8914

Index : Harvard, Boston, Sydney University, Dimensions, Lens, Scilit, Semantic, Google, etc

https://doi.org/10.58578/MJAEI.v2i2.6404

Performance Comparison of Tilt Integral Derivative (TID) Controller and Proportional Integral Derivative (PID) Controller for Parabolic Dish Antenna System

Obi Mathias Inah[1], D. M. Nazif[2], Sadik Umar[3], Fatima Muhammad[4], Yakubu Barau Bal.[5]
Federal Polytechnic Bauchi, Bauchi State, Nigeria
mdnazifi.eeet@fptb.edu.ng

Article Info:

Submitted:	Revised:	Accepted:	Published:
May 22, 2025	Jun 20, 2025	Jul 1, 2025	Jul 6, 2025

Abstract

This study presents a comparative performance analysis of Proportional-Integral-Derivative (PID) and Tilt-Integral-Derivative (TID) controllers in the context of azimuth positioning for a parabolic dish antenna system. A detailed system model was developed in MATLAB/Simulink, integrating key components such as motor dynamics, amplifier behavior, potentiometer-based feedback, and gear mechanisms. The performance of both controllers was evaluated under ideal conditions and in the presence of environmental disturbances, with wind effects modeled using the Dryden wind turbulence model to simulate real-world scenarios. Key performance metrics, rise time, settling time, overshoot, and steady-state error were used to assess controller efficacy. The results indicate that the PID controller outperforms the TID controller in terms of stability, accuracy, and resilience to disturbance. Although the TID controller exhibited a marginally faster initial response, it suffered from greater overshoot and reduced stability, particularly under wind-induced disturbance. These findings underscore the robustness and suitability of PID control for high-precision antenna positioning systems, while also

suggesting that enhancements to TID control may be possible through optimization techniques or hybrid controller designs.

Keywords: PID; TID; Antenna Control; Performance Evaluation; Disturbance Rejection

INTRODUCTION

Satellite antennas are an important component of communication systems. Large amounts of data representing telephone traffic, radio signals, and television signals are carried by satellites. The application of satellite has become increasingly common and has turned out to be an essential part of everyday life, as can be seen in several homes and offices with different forms of antennas which are used for signal reception from satellites located far distance away from the earth (Asiegbu et al., 2021).

To achieve cost effectiveness in receiving satellite transmission data from specific angles, a compensator (controller) is added to the existing antenna system. This subsystem improves performance by providing necessary commands, ensuring stability, steady state, improved transient responses, cost, and robustness. This design applies to designing antenna servo control systems for satellite ground stations (Ekengwu et al., 2021).

Position control systems have, in recent years, been used extensively in applications such as robotics, antennas, automation, and many others. Amongst the most common and traditional techniques for position control are the Tilt Integral Derivative (TID) controller and Proportional-Integral-Derivative (PID) controller. Its straightforward configuration makes it easy to comprehend, and its satisfactory performance causes it to maintain its status as the most widely used controller in the industrial control system. However, the major challenges with the use of conventional PID are the tuning of the parameters and the effect of non-linearity in the plant (Yakubu et al., 2020).

This thesis is about the performance comparison of TID and PID controllers for a parabolic dish antenna system. A technique that incorporates the concepts of both the TID and PID control is explored (Kishore et al., 2020).

Parabolic dish antenna systems are integral to applications such as satellite communications and deep-space exploration, necessitating precise positioning mechanisms to maintain optimal alignment with target sources. Achieving high precision and stability in

these systems is challenging due to inherent nonlinearities, environmental disturbances, and dynamic operating conditions (Shan et al., 2022). However, the emergence of Tilt-Integral-Derivative (TID) controllers offers a promising alternative, potentially providing improved performance in specific scenarios (Kumar, 2023).

The Proportional-Integral-Derivative (PID) controller is a classical control strategy widely employed in antenna positioning systems for its simplicity and effectiveness. However, conventional PID controllers often face limitations in addressing complex nonlinear dynamics and disturbances inherent in parabolic dish antenna systems (Bello et al., 2021).

TID controllers, incorporating tilt and integral-derivative actions, have been proposed as alternatives to traditional PID controllers. Research comparing the performance of PID and TID controllers in various applications suggests that TID controllers can offer superior performance in certain scenarios. For example, (Koszewnik, 2021) Indicated that TID controllers outperformed traditional PID controllers in terms of system stability and response time.

Asiegbu et al., (2021) Utilized a Two-Phase Hybrid Stepping Motor (TPHSM) to control the antenna's azimuth and elevation, aiming for precise line-of-sight alignment with satellites. The study developed a full state feedback controller for an antenna positioning system, improving its performance and efficiency in satellite communication. However, it lacks real-world challenges and requires experimental validation for practical application.

Ekengwu et al., (2021) Examines the impact of various control strategies on the performance of dish antenna positioning systems used in mobile telemedicine applications. The authors developed dynamic equations for a dish antenna position control system, comparing it to existing PID controllers. They developed a full state feedback controller, outperforming PID-based controllers, demonstrating superior transient response characteristics for mobile telemedicine nodes.

Yakubu et al., (2020) Addresses the challenge of enhancing the pointing accuracy of deep space antennas through the implementation of a Fuzzy-PID control technique. The study developed three controllers for controlling the deep space antenna azimuth position using MATLAB and Simulink. The Fuzzy-PID controller significantly improved system performance, outperforming PID and Fuzzy Logic. However, practical challenges like environmental disturbances and hardware limitations remain unaddressed.

Kishore et al., (2020) Presents a comparative analysis of Proportional-Integral-Derivative (PID) and Tilt-Integral-Derivative (TID) controllers applied to a magnetic levitation (maglev) system. The study developed PID and TID controllers for a nonlinear maglev system using Genetic Algorithm and Grey Wolf Optimization. Simulations showed superior performance for the TID controller, but the study lacks experimental validation and real-time implementation feasibility.

Ajiboye et al., (2019) Examines the impact of implementing a Proportional-Integral-Derivative (PID) controller on the positioning performance of dish antennas mounted on mobile telemedicine units in Nigeria. Researchers developed a PID controller for an antenna positioning system, improving performance metrics and responsiveness. Simulations showed a 50.5% overshoot percentage, suggesting further tuning of PID parameters for real-world telemedicine scenarios.

Koszewnik, (2021) Present a systematic procedure for implementing fractional controllers using fractional calculus operators on a Field Programmable Gate Array (FPGA) within the LabVIEW environment. Fractional-order controllers on FPGA hardware offer enhanced flexibility and precision in industrial process control, but further investigation is needed for full-scale industrial systems. (Mahmood et al., 2024) Investigate the effectiveness of three fuzzy logic control (FLC) strategies in enhancing the accuracy of antenna azimuth positioning systems.

Kumar, (2023) Presents a novel approach to Load Frequency Control (LFC) in multi-area interconnected power systems. The authors design a Tilt Integral Derivative (TID) controller to address LFC in a restructured power system environment using the Hunger Games Search (HGS) algorithm. Simulation results show the HGS controller enhances system frequency stability, but lack experimental validation.

The study by Akwukwaegbu et al., (2023) Presents a Model Following Control (MFC) approach integrated with a PID controller (MFC-PID) to enhance the performance of a DC servomotor-based antenna positioning system. Dynamic modeling, frequency domain MFC-PID design, and simulations improve stability and positioning errors in PID controllers, but challenges in handling non-linearity and adaptability suggest the need for further research.

The study by Uthman and Sudin, (2018) Analyzes the performance of two controllers—Proportional-Integral-Derivative (PID) and state-feedback—in managing the

azimuth positioning of antennas. The state-feedback controller outperformed the PID controller in MATLAB/Simulink simulations, offering superior azimuth positioning control for antennas due to shorter settling times and minimal overshoot.

Nantim et al., (2025) Implemented and evaluated an Exponential Rate Reaching Law-based PID (ERPID) controller for a parabolic dish antenna system to improve performance under both normal and disturbed (wind turbulence) conditions. Researchers simulated antenna system dynamics using PID and ERPID controllers, finding ERPID controllers more suitable for precision-critical applications, but lacking real-world validation. Future research should explore adaptive or AI-based control methods.

MATERIALS AND METHODS

Dynamics of the Parabolic Antenna

The control system for parabolic antennas is a complex architecture designed to ensure precise and efficient operation of the antenna in various conditions. At its core is the Antenna Controller Unit (ACU), which serves as the system's brain. The ACU processes user inputs and sensor feedback to generate commands for motor drives responsible for azimuth and elevation adjustments. These motor drives enable the antenna to accurately track targets by moving them horizontally and vertically. Sensors such as encoders and inclinometers provide real-time data on the antenna's position and environmental factors like weather conditions, crucial for the ACU's algorithms to calculate precise adjustments. (Uthman, 2019).

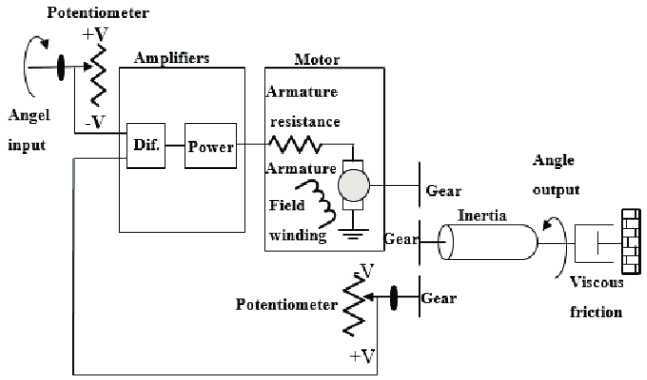

Figure 1: Schematic Diagram of the Parabolic Antenna Control System (Nise, 2015).

PID controllers are essential for accurate pointing and tracking of parabolic antennas, integrating target coordinates, environmental variables, and sensor feedback for optimal performance across various operational scenarios (Ekengwu et al., 2020).

A space antenna position control system is shown with a more detailed schematic (Figure 1) and block diagram (Figure 2).

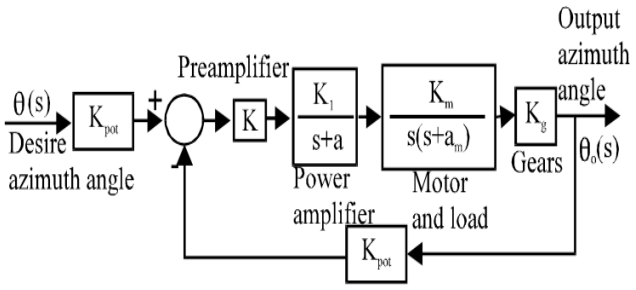

Figure 2: Block Diagram of the Parabolic Antenna Control System (Nise, 2015)

Table 1: Definition of Terms in Antenna Subsystems (Nise, 2015).

Subsystem	Input	Output
Input potentiometer	Angular rotation from a user, $\theta_i(t)$	Voltage to preamp, $v_i(t)$
Preamp	Voltage from potentiometers, $v_e(t) = v_i(t) - v_0(t)$	Voltage to power amp, $v_p(t)$
Power amp	Voltage from preamp, $v_p(t)$	Voltage to motor, $e_a(t)$
Motor	Voltage from power amp, $e_a(t)$	Angular rotation to load, $\theta_0(t)$
Output potentiometer	Angular rotation from load, $\theta_0(t)$	Voltage to preamp, $v_0(t)$

The physical structure of the antenna (including thermal deformations, gravity distortions, encoder mounting, and wind gusts), the control algorithm (software), and the quality of the antenna drives (hardware) all affect pointing accuracy and make it difficult to stay within the necessary pointing-error budget. This system is expected to have the antenna's azimuth angle output, $\dot{\Theta}o(t)$, following the potentiometer's input angle, $\Theta_i(t)$ (Yakubu et al., 2020).

Figure 2 is a block diagram of the system that describes how the system works. The system uses a potentiometer to transform angular displacement into voltage, with the output voltage influenced by the input-output voltage differential, thereby enhancing the motor's rotation speed. There are 5 subsystems of the overall antenna position system, each with its associated transfer function as shown below.

Input and Output Potentiometer

The transfer functions of the input and output potentiometers will be identical because they are configured similarly. To demonstrate the connection between the input angular displacement and the output voltage, the potentiometer dynamics are disregarded. The block diagram of the potentiometer is shown in Figure 3.

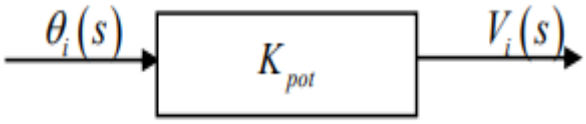

Figure 3: Block Diagram of Potentiometer

The transfer function is given in Equation 1.

$$\frac{V_i(s)}{\theta_i(s)} = K_{pot_i} \quad \text{...(1)}$$

Where: $V_i(s)$ Is the voltage from the input potentiometer [V]; $i_i(s)$ is the input angle [rad]; K_{pot} is the potentiometer gain; N is the number of turns of the potentiometer

Preamplifier

The preamplifier increases the signal input voltage before the power amplifier, with adjustable gain to achieve the desired output. It amplifies input voltage by a specified gain K. Consequently, the equation representing this process is quite straightforward, as illustrated in Equation 2.

$$\frac{V_p(s)}{V_e(s)} = K \quad \text{…(2)}$$

Where $V_p(s)$ is the output voltage of the preamplifier [V]; $V_e(s)$ is the voltage after the summation [V]; K is the preamplifier gain

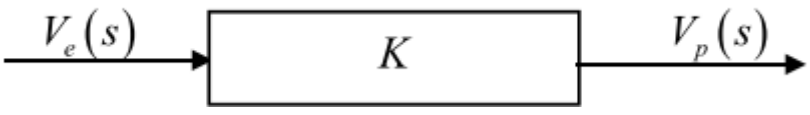

Figure 4: Block Diagram of Preamplifier

Power Amplifier

The third subsystem consists of a power amplifier that converts the output voltage from the preamplifier into a voltage suitable for the motor. The power amplifier type is specified in the design schematic and the associated block diagram.

$$\frac{E_a(s)}{V_p(s)} = \frac{K_1}{s+a} \quad \ldots(3)$$

Where E_a (s) is the power amplifier's output voltage [V]; V_p (s) is the input voltage of the power amplifier from the preamplifier [V]; K_1 is the power amplifier gain; a is the power amplifier pole

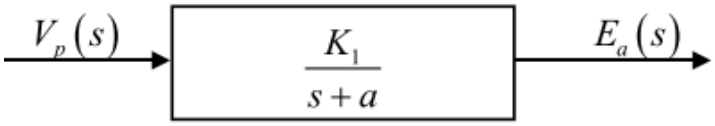

Figure 5: Block Diagram of Power Amplifier

Motor and Load

Following the Power Amplifier is the motor, which connects to the gears and load, in this instance, an antenna. Each of these components must be considered when calculating the transfer function of the mechanical system that results. It is presumed that the motor is a DC servo motor controlled by the armature. This conclusion arises from the motor having a fixed field, which also makes the motor's control simpler.

To obtain the transfer function of the subsystem, it is necessary to establish the equation based on Kirchhoff's Voltage Law (KVL) that connects the input voltage supplied to the motor with the armature's output position (Eze, 2021). The general circuitry of a motor is illustrated in Figure 6.

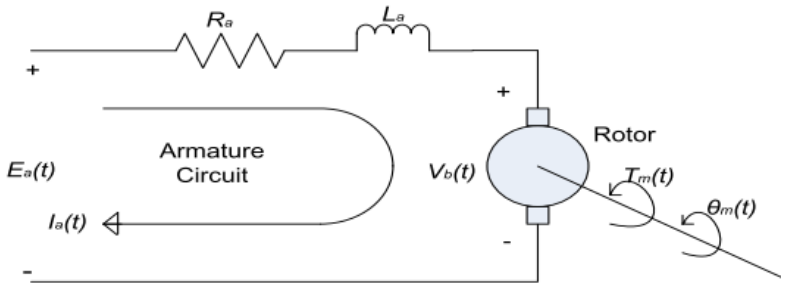

Figure 6: Circuit of a motor (Eze, 2021)

The KVL equation obtained is presented in Equation 3.4. Our focus is solely on the input voltage, and since we lack information about the current input, it would be beneficial to substitute the current term I_a with its corresponding Torque term, as indicated in Equation 3.5.

$$R_a I_a(s) + L_a s I_a(s) + V_b(s) = E_a(s) \quad \text{…..(4)}$$

$$T_m(s) = K_t I_a(s)$$

$$I_a(s) = \frac{T_m(s)}{K_t} \quad \text{….(5)}$$

Where R is the motor resistance [ohms]; I_a is the circuit current [A]; L_a is the motor inductance [H]; V_b (s) is the voltage across the rotor (back EMF) [V]; E_a (s) is the voltage across the motor [V]; T_m (s) is the motor toque [N.m]; K_t is the motor torque constant [N-m/A]

This leads to an equation that lacks a current component but instead features a motor torque. This torque component can be substituted with a term that connects torque to motor speed, position, inertia, and damping. Additionally, one can replace the back EMF term, V_b, with a term that connects back EMF to the speed derivative, which relates to position—a term we will need for constructing the transfer function. Both are presented in equations 6 and 7.

$$V_b(s) = K_b s \theta_m s \quad \text{…(6)}$$

$$T_m(s) = (Js^2 + D_m s)\theta_m(s) \quad \text{…(7)}$$

Where K_b is the back EMF constant [V-s/rad]; θ_m(s) is the angle of rotation of the rotor [rad]; J is the inertial constant [Kg-m^2]; D_m is the dampening constant [N-m s/rad].

Hence, by substituting the related variables with their corresponding values in equation 7 and simplifying, we arrive at equation 8.

$$\frac{(Js^2+D_m s)(R_a+L_a s)\theta_m(s)}{K_t} + K_b s \theta_m(s) = E_a(s) \quad \text{…(8)}$$

This approach is based on the premise that the motor operates in a fixed field, resulting in K_b and K_t being the same. Consequently, extending to the exterior $\theta_m(s)$ produces equation 9.

$$\left[\frac{(Js^2+D_m s)(R_a+L_a s)\theta_m(s)+K_b K_t s}{K_t}\right] \theta_m(s) = E_a(s) \quad \text{…(9)}$$

If $R_a >> L_a$, one can further simplify to equation 10.

$$\frac{\theta_m(s)}{E_a(s)} = \frac{\frac{K_t}{JR_a}}{s\left(s+\frac{D_m R_a + K_b K_t}{JR_a}\right)} \quad \ldots(10)$$

The motor is linked to the damping and inertial elements of the system via a series of gears. This arrangement alters their effective values from the motor's perspective and requires compensation. Compensation can be achieved by applying equations 12 and 13. The ratios of the gears are presented in equation 11.

$$K_g = \frac{N_1}{N_2} \quad \ldots(11)$$

$$J = J_a + J_L\left(K_g\right)^2 \quad \ldots(12)$$

$$D_m = D_a + D_L\left(K_g\right)^2 \quad \ldots(13)$$

Where K_g is gear ratio; N is gear teeth; J_a is the motor inertial constant [kg-m^2]; J_L is the load inertial constant [kg-m^2]; D_a is motor dampening constant [N-m s/rad]; D_L is load dampening constant [N-m s/rad]

Equation 13 matches the transfer function for the motor and load, allowing us to relate the variables K_m and a_m. Their computed values are presented in equations 14 and 15.

$$K_m = \frac{K_t}{JR_a} = \frac{1}{0.25x5} \quad \ldots(14)$$

$$a_m = \frac{D_m R_a + K_b K_a}{JR_a} \quad \ldots(15)$$

Where K_m is motor and load gain m; a_m is motor and load pole.

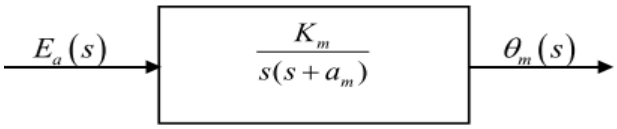

Figure 7: Motor, Load, and Gears

The PID Controller

A controller minimizes the error between a measured process variable and a reference by calculating the error and generating a correction signal. Automatic controllers compare the output with the desired value, determine deviation, and produce a control signal (Bankole, 2022). Proportional Integral Derivative (PID) controllers provide feedback, eliminate steady-state offsets, and anticipate futures. They are widely used in

industrial processes due to their simplicity, design, low maintenance, effectiveness, stability, and reliability. Figure 8 explains the PID controller.

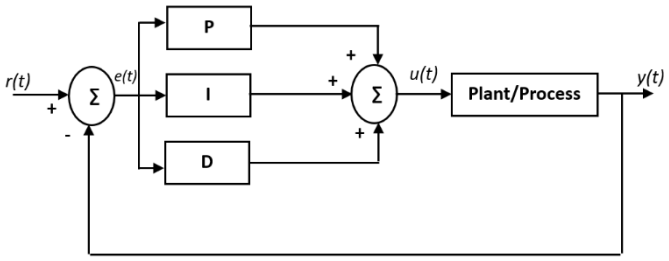

Figure 8**:** PID Controller

An automatic controller detects and amplifies an actuating error signal, feeding it to an actuator like an electric motor. The actuator produces input to the plant, ensuring the output approaches the reference input signal (Bankole, 2022). A sensor converts the output variable into a suitable variable, comparing it to the reference input. The controller's set point must be converted to the same units as the feedback signal.

The Proportional, Integral, and Derivative components work together additively to form the PID Controller. The P-controllers, PI-controllers, or PD-controllers are frequently used because not all of them must be present; any other version can be obtained by removing the unnecessary components.

The PID controller's function relies on the computation of the "tracking error" e(t) and its three gains K_p, K_i, and K_d. In their combination, they lead to the control action u, as shown in the following expression:

$$u(t) = K_p e(t) + K_i \int e(t)\, dt + K_d \frac{de}{dt} \qquad \ldots(16)$$

Where K_p = proportional gain, K_i = integral gain, K_d = derivative gain, e(t) = error at the current time, and t = integration variable.

The first term on the right side is the proportional term, the second is the integral action, and the final term is the derivative. Each of these parameters has a unique influence on the closed-loop system's transient and steady-state responses.

The P-action is crucial for a system's dominant reaction, resulting in shorter rise times but larger overshoots. The derivative action adjusts damping behavior, causing larger steady-state errors and smaller overshoots. The integral action optimizes steady-state

response and dynamic behavior, providing system memory. Increasing gain KI leads to greater oscillations but reduced steady-state errors.

TID Controller

The Tilt Integral Derivative (TID) controller is a feedback-type controller, similar to the PID controller and with the same advantages, while also having greater dynamic properties. Both controllers have identical integral and derivative actions, but the proportional action of the PID controller is replaced with a tilt-proportional controller with internal feedback (Kumar, 2023). This is shown in Figure 9.

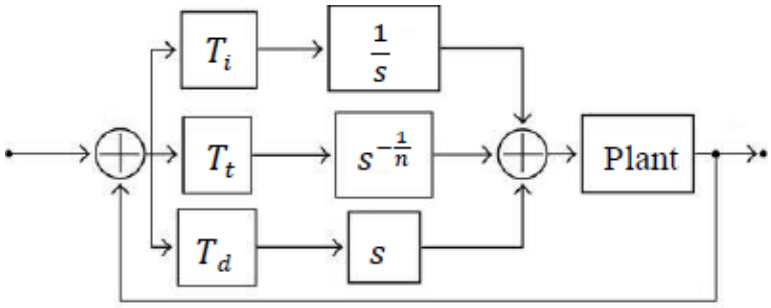

Figure 9: TID Controller

Tilt- Integral-Derivative Controller Structure. Figure 9 depicts the structure of a TID controller. It has a PID controller-like configuration, with the proportional element tilted due to the $s^{-1/n}$ transfer function. It allows for easier tuning, improved disturbance rejection, and increased sensitivity to changes in system parameters (Naik et al., 2024)

Equation (14) is the transfer function expression of a TID controller, respectively.

$$TF/_{TID} = K_t S^{\frac{-1}{n}} + \frac{K_i}{S} + K_d S \qquad \text{----(17)}$$

Where K_t = tilt gain, K_i = integral gain, K_d = derivative gain, and s = integration variable.

Disturbance

Wind disturbance is one of the most important disturbances to consider in antenna positioning control (Chandra et al., 2021). Wind disturbance (Wind Gust) is a critical factor that needs to be considered in the control system design for parabolic dish antennas. External wind forces can significantly affect the antenna's precise pointing accuracy, causing undesirable movements and deviation from the desired target (Wajirakumara, 2021).

In this research, the wind disturbance was modeled as a time-varying torque input to the dynamic antenna system. The wind force can be represented as a stochastic process, with its characteristics based on historical data or assumed scenarios to assess the controller's robustness.

For more accurate modeling, especially in high-wind scenarios, it can be helpful to model wind as a stochastic process to simulate gusts or fluctuations. A commonly used model for turbulent wind is the Dryden wind turbulence model, which captures the variability and frequency content of wind disturbances (Harris, 2020).

The Dryden model characterizes wind as a first-order system responding to random inputs, with the wind speed $V_{wind}(t)$ modeled (Tan et al., 2020) as:

$$\dot{v}_{wind}(t) = -\frac{1}{L} v_{wind}(t) + W(t) \quad \ldots(18)$$

Where L is the turbulence scale length (typically around 10–30 meters, depending on the location and height); W(t) is the white noise process representing random wind fluctuations.

In this case, $v_{wind}(t)$ is a stochastic process that varies over time, simulating realistic wind patterns. The resulting torque $T_{wind}(t)$ then becomes:

$$T_{wind}(t) = \frac{1}{2} C_d \rho A v_{wind}(t)^2 \quad \ldots(19)$$

where: C_d is the Drag coefficient, a dimensionless factor depending on the antenna's shape and orientation; ϱ is the Air density (approximately 1.225 kg/m³ at sea level); A is the Effective surface area of the antenna facing the wind; $v_{wind}(t)$ is the Instantaneous wind speed (m/s).

Through simulation studies, the performance of the TID controller was evaluated and compared to a traditional PID controller under various wind disturbance scenarios. The metrics of interest will include the antenna's tracking accuracy, settling time, and the ability to reject wind-induced disturbances.

RESULTS AND DISCUSSION

Step Response of an Antenna Position Control System without Disturbance

The first sets of simulations were carried out to observe the response of the antenna positioning system under ideal conditions, that is, without any external disturbance. The results demonstrate how each controller tracks the reference signal. The PID controller output closely follows the reference input with minimal overshoot. Conversely, the TID controller shows a faster initial rise but exhibits significant overshoot before settling.

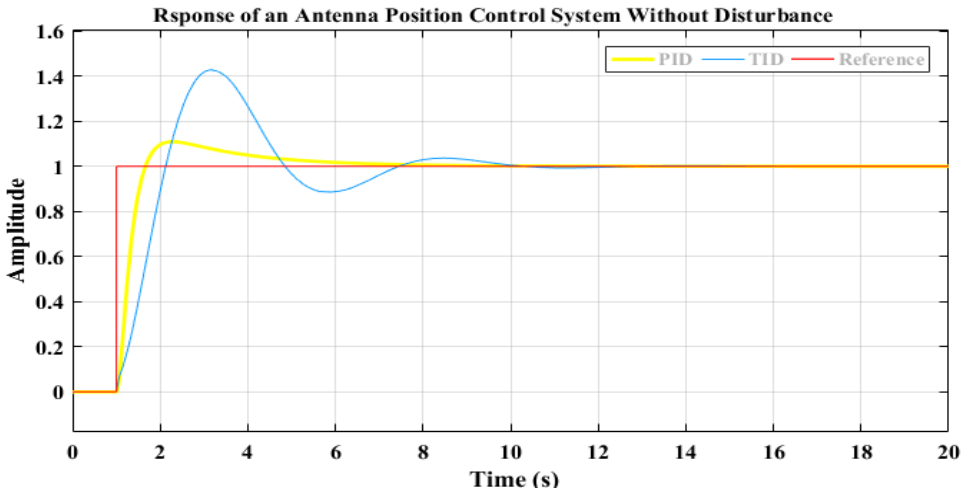

Figure 10: Step Response of an Antenna Position Control System without Disturbance

Step Response of an Antenna Position Control System with Disturbance

The second phase of the simulation introduced external disturbances to test the robustness of both controllers. In this scenario, PIDWD and TIDWD represent the PID and TID controllers operating under disturbance, respectively. Figure 4.2 shows the system response when a disturbance is introduced. The PIDWD controller effectively maintains stability and tracks the reference input with minimal fluctuation. In contrast, the TIDWD controller displays significant oscillation before settling.

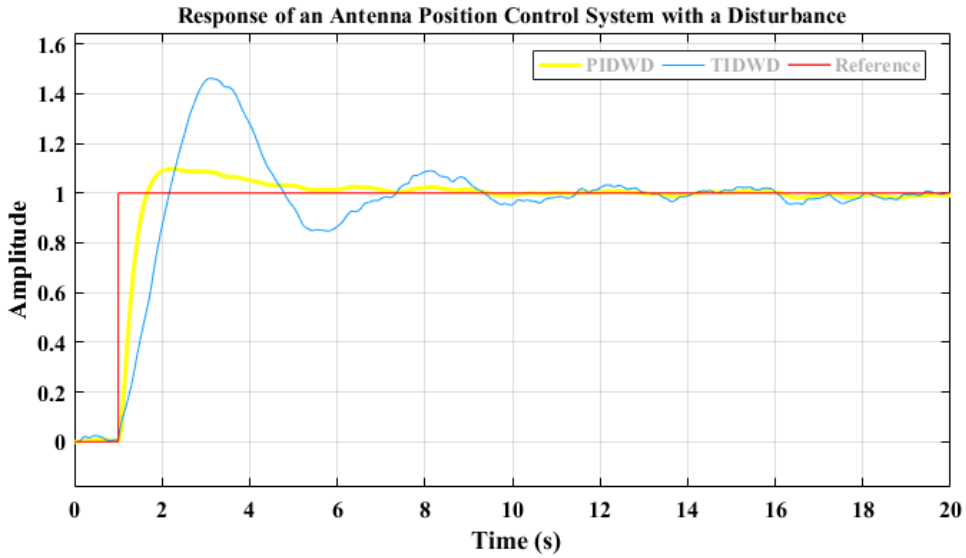

Figure 11: Step Response of an Antenna Position Control System with Disturbance

The overall results from both scenarios are summarized in Table 2.

Table 2: Controllers' Performance Results

Parameters	PID	PID-WD	TID	TID-WD
Rise Time (s)	0.4820	0.3200	0.7111	0.6667
Settling Time (s)	6.9700	6.9800	6.5400	6.9050
Overshoot (%)	150	66.6667	800	500
Steady-State Error	0.000421	0.005905	0.002882	0.002033

From Table 2, the simulation results comparing the PID and TID controllers for the parabolic dish antenna system revealed distinct performance differences under both ideal (without disturbance) and disturbed conditions. Without disturbance, the PID controller exhibited a very low steady-state error of 0.000421, a rise time of 0.4820 seconds, a settling time of 6.9700 seconds, and an overshoot of 150%, indicating quick and accurate tracking. In contrast, the TID controller recorded a higher error of 0.002882, a slower rise time of 0.7111 seconds, a settling time of 6.5400 seconds, and a significantly larger overshoot of 800%, reflecting instability in its initial response despite its faster convergence. When disturbances were introduced, the PIDWD (PID with disturbance) still maintained commendable performance with an error of 0.005905, a much faster rise time of 0.3200 seconds, a settling time of 6.9800 seconds, and a moderate overshoot of 66.67%. The TIDWD (TID with disturbance) controller had a lower error of 0.002033 but experienced a longer rise time of 0.6667 seconds, settling time of 6.9050 seconds, and an

extremely high overshoot of 500%, which could cause instability in real applications, especially in an antenna positioning system. These results clearly show that while TID controllers may offer slightly better error values in disturbed environments, the PID controller consistently provides more balanced performance across all metrics, making it a more reliable choice for antenna tracking systems that require both accuracy and robustness.

CONCLUSION

This study investigated the performance of Proportional-Integral-Derivative (PID) and Tilt-Integral-Derivative (TID) controllers in the positioning control of a parabolic dish antenna system. The evaluation was carried out under different scenarios: one without disturbance and another with the introduction of external disturbance. The simulation results revealed that the PID controller consistently provided better performance compared to the TID controller. Specifically, the PID controller demonstrated minimal steady-state error, reduced overshoot, and faster settling time, especially under disturbed conditions. Its ability to closely track the reference signal and maintain stability under varying circumstances made it the more reliable option. On the other hand, the TID controller, while showing a slightly quicker initial response in some cases, suffered from significantly higher overshoot and was less effective in handling disturbances. The results suggest that the PID controller is more suitable for applications that require precision and robustness, such as antenna tracking systems.

The research suggests improving the TID controller's performance using optimization techniques like Genetic Algorithms or Particle Swarm Optimization. A hybrid control strategy combining PID and TID features could be developed. Practical implementation of these controllers on a physical parabolic antenna system is also recommended, considering noise, actuator limitations, and hardware non-linearity.

REFERENCES

Ajiboye, A. T., Ajayi, A. R., & Ayinla, S. L. (2019). Effects of PID controller on the performance of dish antenna position control for distributed mobile telemedicine nodes. *ATBU Journal of Environmental Technology*, *15*(2), 304–313. Retrieved from http://www.azojete.com.ng

Akwukwaegbu, I. O., Chikezie, N. O., Olubiwe, M., Francis, P. N. C., & Okoronkwo, E. (2023). Design of model following control integrating a PID controller for a DC servomotor-based antenna positioning system. *SSRG International Journal of Electrical and Electronics Engineering*, *10*(6), 33–42. https://doi.org/10.14445/23488379/IJEEE-V10I6P104

Asiegbu, N. C., Udechukwu, C. F., & Ekennodu, C. (2021). Antenna positioning control system for effective satellite communication. *International Journal*, *4*(12), 27–34.

Bankole, A. T. (2022). A novel hybrid proportional derivative / H-infinity controller design for improved trajectory tracking of a two-link robot arm. *International Journal*.

Bello, Á., del Castañedo, Á., Olfe, K. S., Rodríguez, J., & Lapuerta, V. (2021). Parameterized fuzzy-logic controllers for the attitude control of nanosatellites in low Earth orbits: A comparative study with PID controllers. *Expert Systems with Applications*, *174*, 114679. https://doi.org/10.1016/j.eswa.2021.114679

Chandra, M., Kumar, S., Chattopadhyaya, S., Chatterjee, S., & Kumar, P. (2021). A review on developments of deployable membrane-based reflector antennas. *Advances in Space Research*, *68*(9), 3749–3764. https://doi.org/10.1016/j.asr.2021.06.051

Ekengwu, B. O., Mbachu, C. B., & Nwabueze, C. A. (2020). Design of PID-tuned digital compensator for improved positioning performance of satellite dish antenna for distributed mobile telemedicine nodes within Nigeria. *Journal of Control*, 117–123.

Ekengwu, B. O., Mbachu, C. B., Nwabueze, C., & Akaneme, S. A. (2021). Effect of different controllers on the performance of the dish antenna positioning system for distributed mobile telemedicine nodes. *ResearchGate*. https://doi.org/10.13140/RG.2.2.30349.05606

Eze, P. C. (2021). Positioning control of DC servomotor-based antenna using PID tuned compensator. *Journal of Engineering Sciences*, *8*(1), 8–16. https://doi.org/10.21272/jes.2021.8(1).e2

Harris, J. L. (2020). Characterization and sensitivity analysis of 6-meter Cassegrain antenna. *Research Paper*.

Kishore, S., Pandey, N., Kumar, V., & Raj, A. (2020). Performance comparison of PID and TID controllers using genetic algorithm and grey wolf optimization technique for magnetic levitation system. *IOSR Journal of Electrical and Electronics Engineering*, *10*(6), 1–9. https://doi.org/10.9790/9622-1006040109

Koszewnik, A. (2021). Experimental studies of the fractional PID and TID controllers for industrial processes. *International Journal*, *19*(5), 1847–1862.

Kumar, S. A. (2023). Application of a TID controller for the LFC of a multi-area system using the HGS algorithm. *International Journal*, *13*(3), 10691–10697.

Mahmood, A., Al-Bayati, K. Y. A., & Szabolcsi, R. (2024). Optimizing antenna azimuth position control using fuzzy PD, fuzzy PD-I, and fuzzy PD-plus-I controllers. *Nano NTP*, *20*(3). https://doi.org/10.62441/nano-ntp.v20i3.2

Naik, A. K., Jena, N. K., Sahoo, S., & Sahu, B. K. (2024). Optimal design of fractional order tilt-integral derivative controller for automatic generation of power system integrated with photovoltaic system. *Electrica*, *24*(1), 140–153. https://doi.org/10.5152/electrica.2024.23044

Nantim, J., Mohammed, A., Sadiq, A. A., Nazif, D. M., & Bauchi, F. P. (2025). Investigation on the implementation of the exponential rate reaching law on the parabolic dish antenna system. *Asian Journal*, *3*(2), 300–318.

Nise, N. S. (2015). *Control systems engineering* (7th ed.). John Wiley & Sons.

Shan, Y., Xia, L., & Li, S. (2022). Design and simulation of a satellite attitude control algorithm based on PID. *Journal of Physics: Conference Series*, *2355*(1). https://doi.org/10.1088/1742-6596/2355/1/012035

Tan, N. D., Giang, L. N., & Viet, N. D. (2020). Modelling and simulation of a hexapod antenna system for tracking VNREDSAT-1 satellite. In the *2020 IEEE International Conference on Environment and Electrical Engineering and the 2020 IEEE Industrial and Commercial Power Systems Europe (EEEIC/I&CPS Europe)*. https://doi.org/10.1109/EEEIC/ICPSEurope49358.2020.9160586

Uthman, A. (2019). Antenna azimuth position control system using model reference adaptive control method, gradient approach, and stability approach. *Journal of Engineering and Applied Sciences*, *14*(16), 5657–5664.

Uthman, A., & Sudin, S. (2018). Antenna azimuth position control system using PID controller & state-feedback controller approach. *International Journal of Electrical and Computer Engineering*, *8*(3), 1539–1550. https://doi.org/10.11591/ijece.v8i3.pp1539-1550

Wajirakumara, A. (2021). Simulation of precise automatic radio frequency ground station tracking for S-band satellites. *Master's thesis*. Retrieved from http://www.diva-portal.org/smash/record.jsf?pid=diva2:1548727

Yakubu, H., Hussein, S., Koyunlu, G., Ewang, E., & Abubakar, S. (2020). Fuzzy-PID controller for azimuth position control of deep space antenna. *Covenant Journal of Informatics and Communication Technology*, *8*(1), 1–7. https://doi.org/10.47231/rcqk7274